Published in Surface Science 473, issues 1-2, 17-24, 2001
which should be used for any reference to this work

Geometrical and electronic structure of Pd clusters on graphite

M. Bovet [a,*], E. Boschung [a], J. Hayoz [a], Th. Pillo [a], G. Dietler [b], P. Aebi [a]

[a] *Institut de physique, Université de Fribourg, Pérolles, CH-1700 Fribourg, Switzerland*
[b] *Institut de physique expérimentale, Université de Lausanne, CH-1015 Lausanne, Switzerland*

Abstract

Pd clusters formed by physical vapor deposition at room temperature (RT) on highly oriented pyrolytic graphite were investigated by a combination of X-ray photoelectron spectroscopy and diffraction, angle-resolved ultraviolet photoelectron spectroscopy, scanning tunneling microscopy and calculations based on the local density functional theory. Different coverages with nominally 3, 5 and 10 Å were studied after deposition at RT and after heat treatment at 600°C. Local ordering exhibiting growth with an fcc(1 1 1) orientation is already observed at the lowest coverage, but with no preferred azimuthal orientation in accordance with the substrate itself. However electronic structure features characteristic for a Pd(1 1 1) single crystal appear only after heat treatment.

Keywords: Palladium; Graphite; Clusters; Photoelectron diffraction; Angle resolved photoemission; Density functional calculations

1. Introduction

Clusters, formed by vapor deposition onto relatively inert substrates, are of great interest as model systems because of their importance in the field of heterogeneous catalysis and cluster physics. Small supported clusters, especially consisting of Pd, have frequently been investigated by means of photoelectron spectroscopy [1]. Since atomic scale characterization is very important to understand catalytic properties, studies of such systems have been intensified owing to the invention of scanning tunneling microscopy (STM) [2–5]. If clusters are formed by deposition from the vapor phase onto the substrate, their final shape, and thus their properties, are determined by the nucleation mechanism and adsorbate–substrate interaction which are both temperature dependent [6].

In the present paper we investigate the morphology, geometrical and electronic structure of Pd clusters grown on highly oriented pyrolitic graphite (HOPG) by room temperature (RT) evaporation, both, immediately after deposition and after subsequent annealing to 600°C. Sample preparation and experiments have been performed in situ. STM was used to identify the formation of clusters, the geometrical structure was determined by X-ray photoelectron diffraction (XPD) and the electronic bandstructure was observed by angle resolved ultraviolet photoelectron spectroscopy (ARUPS), what, to our knowledge, has not been done so far. The Pd bands were identified via comparison with full potential linearized augmented plane waves (FLAPW) calculations [7].

* Corresponding author. Tel.: +41-26-300-9088; fax: +41-26-300-9747.
E-mail address: marc.bovet@unifr.ch (M. Bovet).

2. Experimental

The experiments were performed in a VG ESCALAB Mk II spectrometer with a base pressure $\leqslant 5 \times 10^{-11}$ mbar. The sample stage is modified for motorized sequential angle-scanned data acquisition over 2π solid angle [8,9]. MgK_α radiation (1254.6 eV) was used for X-ray photoelectron spectroscopy (XPS) in order to check the cleanness of the sample with respect to O1s or to determine intensity ratios between the C1s and the Pd peaks. The data acquisition mode to collect full-hemispherical XPD data is described in detail elsewhere [10]. ARUPS measurements were performed with monochromatized HeI_α radiation (21.2 eV). The setup of the plasma discharge lamp with the monochromator, which is able to separate the different excitation lines from various gases like He, Ne, and H_2, is presented elsewhere [11]. The energy resolution of the analyzer (angular resolution 1° full cone) for the ARUPS measurements was set to 50 meV. STM images were taken with a DME Rasterscope 3000 [12] in constant-current mode. All images were collected using an electrochemically etched W tip.

The HOPG surface was prepared in ultrahigh vacuum by cleaving with adhesive tape. Pd was evaporated at RT by resistive heating of a thin Pd wire wrapped around a Ta filament. The coverage was monitored with a quartz crystal oscillator. After a first characterization following Pd deposition the sample was heated to 600°C (as measured by a pyrometer) for 1 h using resistive heating of a Ta filament inside the sample holder. Thereby, the pressure did not exceed 1×10^{-9} mbar. Note that it is very unlikely that Pd desorbs during this heat treatment since its vapor pressure at this temperature is below 10^{-11} mbar. Before performing the second set of experiments the sample was allowed to cool down for at least 2 h after heating.

3. Results and discussion

STM measurements were carried out to confirm that Pd grows in clusters on the HOPG surface. We believe that Pd grows in clusters on graphite since a hexagonal structure identical to that on a clean graphite can be detected in between the Pd. Fig. 1 shows a set of pictures before and after annealing for all coverages. They show that the clusters become more regular and uniform in size and shape after annealing. [1] In addition at 10 Å, one can see that the annealing process has allowed the formation of large triangular clusters with preferential orientation. Similar ones were found by Kojima et al. [2] after Pd evaporation at 450°C.

XPS intensities of the Pd and the graphite substrate were analyzed. In Fig. 2 the mean ratios between the intensities of the Pd peaks (for statistical reasons, averaging was done over the 3p and 3d intensities of Pd) and the C1s peak are plotted for the different layer thicknesses before (round markers) and after annealing (square markers). We notice a decrease of the ratios after heating. The crossed markers show the mean ratios between the intensity ratios before and after heat treatment. While for the thicker layer (10 Å) the intensity ratios experience practically no change the ones for the thin layers decrease markedly up to a factor of 1.8 (3 Å). Neglecting the possibility of Pd intercalation in HOPG [13], [2] two explanations may be given. Either part of the deposited material desorbs during annealing, which is very unlikely according to the vapor pressure during the heating process, or the clusters after having possibly coalesced, become higher and smaller in diameter. The clusters then cover less surface area and, therefore, the Pd/C intensity ratio decreases. As more Pd is deposited the ratio tends to be less altered, possibly because the clusters have reached a more stable size which does not change anymore after heating the 10 Å deposit.

The local geometric structure of the clusters has been investigated by XPD. Fig. 3 compares the XPD patterns of the three low index faces of fcc single crystals, i.e. the (1 1 1), the (0 0 1), and the

[1] The quality of the STM images is such that it does not allow a systematic, statistical analysis of the cluster size and height. STM is merely used to confirm the presence of clusters.

[2] To our knowledge there is no indication about Pd intercalation in HOPG, see e.g., Ref. [13].

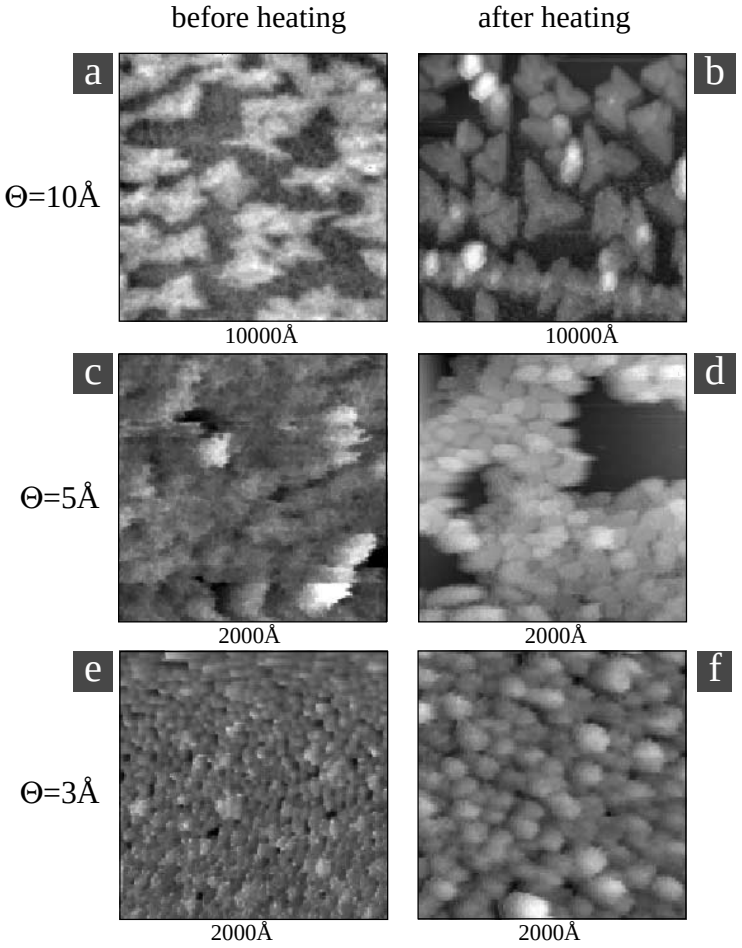

Fig. 1. STM images for Pd coverages, Θ, of 10, 5, and 3 Å on graphite before and after heating. For heating the sample was removed from the STM stage and put back again after cooling down, i.e. the images are measured at different locations on the sample surface. X and Y dimensions are indicated at the bottom. Note the different image sizes between the 10 Å film (a,b) and the other ones. All films show more regular shapes after annealing. All images were collected using the same electrochemically etched W tip.

(1 1 0) surfaces (Fig. 3a), to the diffraction pattern of a 5 Å Pd film after evaporation onto HOPG at RT (Fig. 3b). The different photoemission peaks have been measured as a function of the emission angle and mapped stereographically in a linear grayscale representation. High and low intensities are drawn in white and black, respectively. Normal emission corresponds to the center of the plot whereas emission parallel to the surface, i.e. 90° polar emission angle, is indicated by the outer circle.

XPD allows a very simple interpretation in the case of photoelectron kinetic energies above approximately 500 eV [14]. Photoelectrons leaving the emitter atom are strongly focused in forward direction by the neighboring atoms. The measured intensities are therefore high along densely packed atomic rows and crystallographic planes. In this energy regime, the so-called forward focusing is only weakly dependent on the atomic number Z. Furthermore, it was shown in Ref. [9] based on a large data set that the final-state scattering

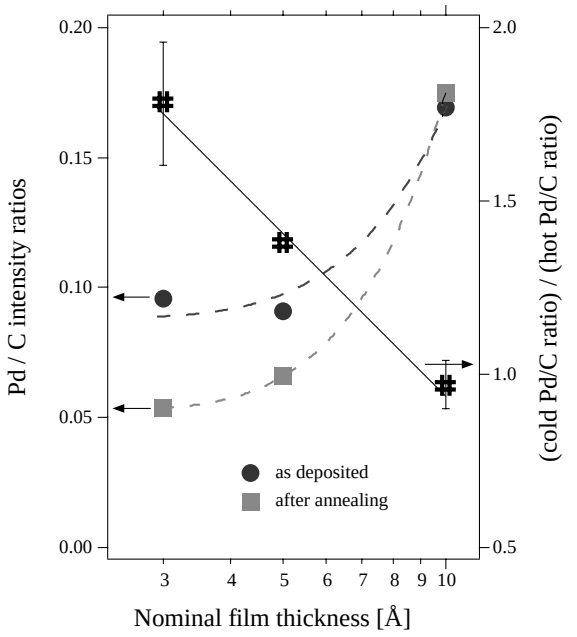

Fig. 2. Palladium to Carbon XPS intensity ratios for the as-evaporated (●) and the annealed Pd on HOPG samples (▒) as a function of the nominal film thickness. Errors are of the size of the markers. Dividing the ratios yields a value (#) that is a measure for the shape change upon heating (see text, error bars are indicated).

produces patterns that are virtually independent of the initial state angular momentum. All four surfaces have been measured at kinetic energies near 1 keV where the high intensity features are almost solely produced by forward focusing of elastically scattered photoelectrons [9]. The position of the maxima thus depends basically only on the local geometric structure and is therefore characteristic for an fcc structure with a particular orientation. The comparison of the Pd signal with previous experiments on Ag and Cu [9,15] is straightforward since all, Pd, Ag, and Cu, crystallize in the fcc structure.

The appearance of rings for the Pd pattern instead of discrete maxima is remarkable. It is due to the azimuthal random orientation of the small graphite microcrystals of the highly textured HOPG surface. The crystallites are only well aligned along the *c*-axis [16]. The C1s XPD pattern of HOPG (not shown here) exhibits therefore only rings as well. However, the intensity distribution along the polar emission angle θ, $I(\theta)$, is still characteristic for only one facet of an fcc surface. In order to investigate this it is useful to plot the azimuthally averaged $I(\theta)$, normalized to the smooth polar angle dependent background to gain a so-called anisotropy [17,18]. As illustrated in Fig. 4a, two fcc(1 1 1) oriented single crystals deliver similar anisotropies, demonstrating their independence on Z. Fig. 4b also shows the similarity of XPD patterns and anisotropies before and after heating. It becomes clear that the anisotropies are quite similar for single crystals and the Pd on HOPG, as deposited and annealed. From this similarity we learn that the amount of unordered Pd on HOPG is negligible.

In Fig. 3c the topmost graph shows the anisotropy of the Pd film and is compared to the corresponding curves for the different fcc surfaces of Fig. 3a. High intensity features for Pd are labeled from A to D. Immediately, fcc(1 1 0) oriented facets can be ruled out. For small θ, i.e. for peaks A and B, the anisotropies for the (1 1 1) and the (0 0 1) facet are similar and both correspond to the Pd film. Peaks C and D, however, clearly demonstrate the (1 1 1) alignment of the Pd film. The features A–D have been observed for all sample preparations, i.e. for all thicknesses before and after annealing. Note that feature A, i.e., a forward focusing maximum in normal emission direction, indicates the presence of at least four Pd layers in the cluster, since consecutive atoms along the (1 1 1) direction occur only every fourth layer. Therefore, at 3 and 5 Å, the clusters appear to be considerably thicker than what is expected from the quartz microbalance, [3] giving an additional indication for the presence of clusters instead of uniform layers.

The behavior for $\theta > 60°$ (see Fig. 3b) can be attributed to the sample fixation on the holder, leading to non-uniform anisotropic features for grazing emission.

Fig. 5a shows angle-scanned energy dispersive curves from normal emission up to 40° polar angle

[3] Four Pd layers in the (1 1 1) direction correspond to a thickness of 6.74 Å.

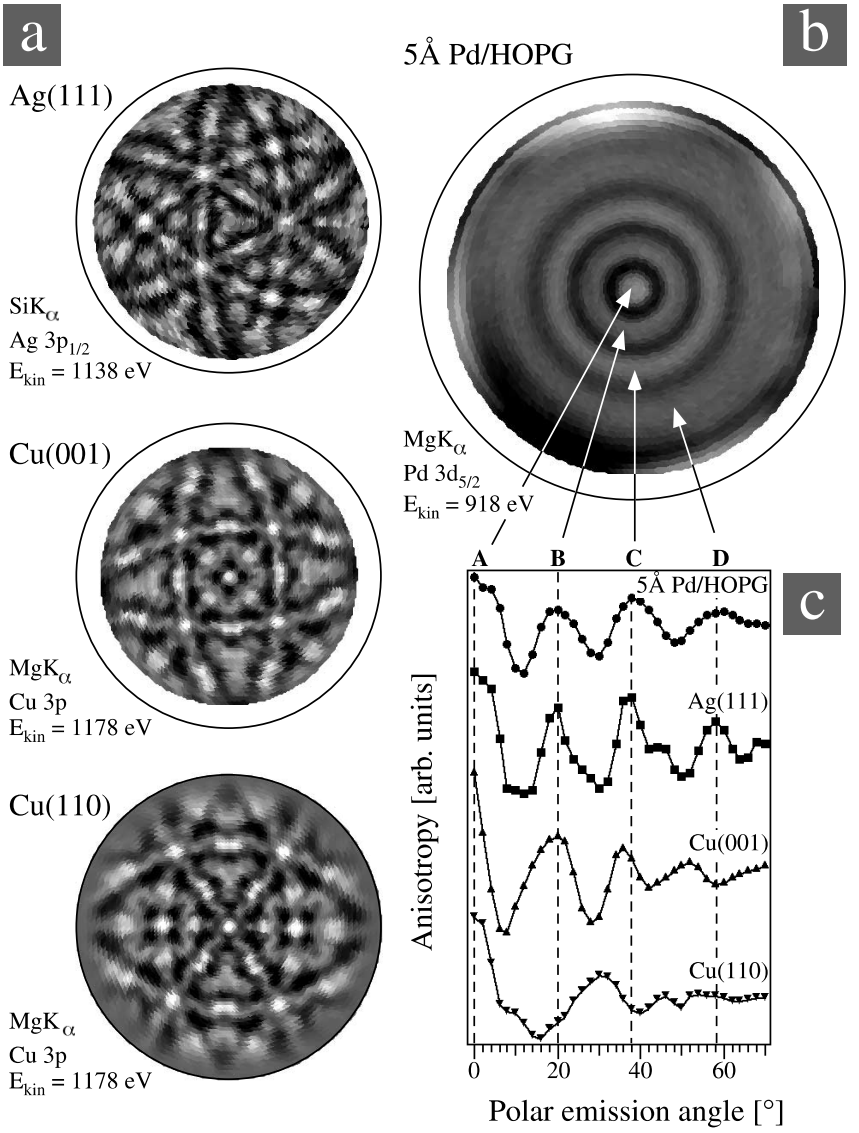

Fig. 3. Comparison of stereographically projected XPD patterns measured (a) on Ag and Cu single crystal surfaces, (b) on 5 Å Pd film on HOPG and (c) anisotropies in azimuthally averaged polar angle cuts. Labels A–D mark the high-intensity features on the Pd evaporated sample.

for clean HOPG and 5 Å Pd on HOPG, before and after heating. They were observed for all thicknesses. The spectra were taken in polar angular steps of 2° using HeI$_\alpha$ radiation (21.2 eV). Linear interpolation in the direction of the angle axis was performed before representation in a grayscale plot. Black means high intensity. Graphite is known to have a low density of states near the Fermi level E_F and it is therefore not astonishing to observe only a part of a band in the lower right corner in our dispersion plot. Evaporation of Pd produces a large bump of apparently localized states between -2 and -3 eV binding energy and an increased spectral weight near E_F. Only by heating, these states become sharper and one can even follow the dispersion of individual bands

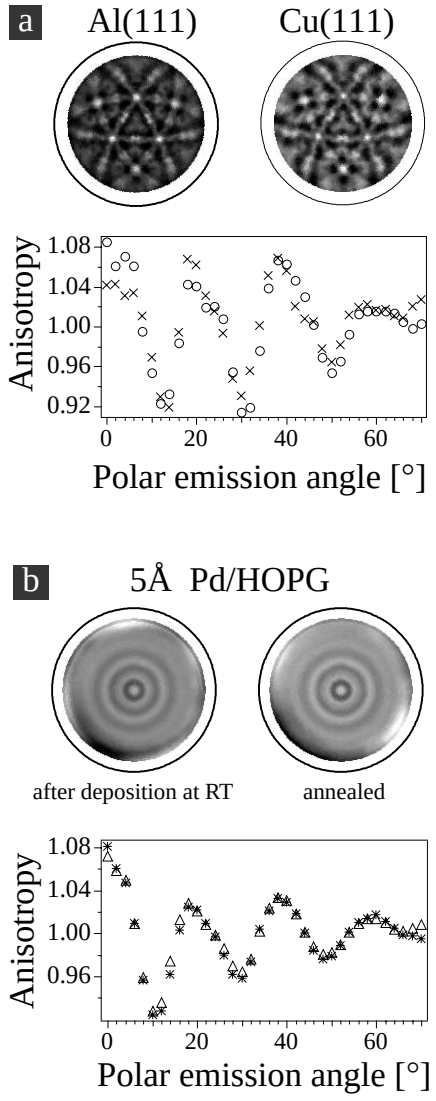

Fig. 4. (a) Stereographically projected XPD patterns of two fcc(1 1 1) oriented single cristals. Cu3p was measured at 1179 eV and Al2s at 1136 eV, both with MgK_α. One can look how similar the anisotropies are for both aluminium (×) and copper (○). (b) Anisotropy and XPD pattern of the 5 Å Pd film on HOPG after deposition at RT (✳) and after the annealing process (△).

from $\theta = 0°$ up to 30° as indicated by the dotted white lines in Fig. 5a.

In order to understand the observed electronic structure we performed bulk band structure 'first principles' calculations of pure Pd based on the density functional theory (DFT) using the FLAPW method [7] within the generalized gradient approximation [19] and assuming a free electron final state. The results are shown in Fig. 5b. Ten, equally spaced polar angle cuts between $\bar{\Gamma} - \bar{M}$ and $\bar{\Gamma} - \bar{K}$ as indicated in the surface Brillouin zone of an fcc(1 1 1) surface have been calculated and added up in order to simulate averaging over the irreducible wedge of the Brillouin zone. For small θ the theoretical cut is in good agreement with the experimental data for the heated sample. On the as-prepared sample only the diffuse feature at -2.5 eV is observed near normal emission. The second peak at -1 eV, characteristic for angle-resolved normal emission spectra of Pd(1 1 1) [20], appears only upon annealing to at least 520°C. For larger θ the Brillouin zone averaging leads to a smeared out density in the electronic structure (see Fig. 5b) and, accordingly, the measured structure becomes diffuse for $\theta > 20°$. The calculated band dispersing downward and starting at normal emission at -3 eV is not present in the experiment. The cluster size (or height) may not be sufficient to produce this feature. Furthermore, our calculations disregard matrix elements. Hence, in order to know whether this is intrinsic to our Pd clusters or an artifact of the calculation it would be necessary to compare with measurements on a Pd(1 1 1) single crystal. These measurements indicate that, although clusters formed by RT evaporation already show a local (1 1 1) ordering, electronic band structure features only show up when the clusters have been heated. This is consistent with the rearrangement of the clustershape upon annealing and possibly the cluster size (or height) is not sufficient to produce the downward dispersing feature starting at -3 eV.

It is possible to speculate that such a locally ordered structure without developed electronic bands might indicate a dendritic aggregation of the Pd particles on the graphite surface as was observed for Au on HOPG [21]. Only after annealing the electronic structure of Pd is observed, suggesting achievement of a long range order. With increasing deposition temperature many epitaxial systems on closed packed substrates reveal a direct transition from dendritic to compact islands. The

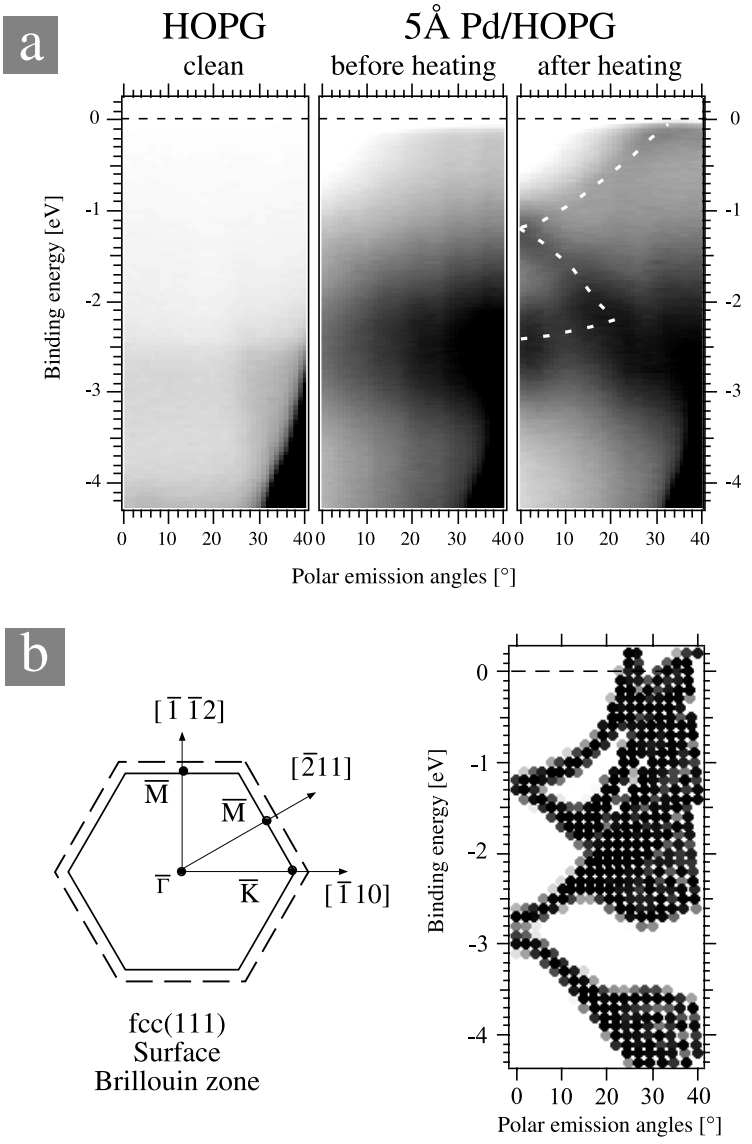

Fig. 5. (a) Grayscale dispersion plots for clean HOPG, 5 Å Pd on HOPG before and after heating. Clear dispersion near E_F appears only after annealing the Pd film. (b) Band structure calculation of bulk Pd adapted to simulate a He I measurement azimuthally averaging over the irreducible wedge of the Brillouin zone between $\bar{\Gamma}-\bar{M}$ and $\bar{\Gamma}-\bar{K}$. The high symmetry axes and points in the surface Brillouin zones of fcc(1 1 1) Pd and HOPG are indicated on the left. The dashed line is the HOPG surface Brillouin zone. The $\bar{K}$ points of the Pd and HOPG Brillouin zones correspond to approximately 47° and 55°, respectively.

compact islands are mostly triangles whose preferred orientation is set by the trigonal symmetry of the dendrites preceding at low temperatures. One of the most spectacular example is Pt/Pt(1 1 1) which exhibits a transition from dendrites to a series of polygonal island shapes [22].

4. Conclusion

In summary, angle-resolved ultraviolet, XPS, and STM have been employed to characterize the geometrical and electronic structure of palladium clusters on pyrolytic graphite. The resulting

clusters have been investigated after RT deposition and after subsequent annealing to 600°C.

STM showed the presence of clusters. XPD demonstrates that at every stage, i.e., before and after heating and at all coverages, the local growth orientation is epitaxial fcc(1 1 1). The heated clusters, as indicated by XPS and STM, get smaller and higher after having possibly coalesced for both first deposits (3 and 5 Å) or just transform into triangular shape at 10 Å. The change in morphology has consequences on the electronic structure of the clusters. The ARUPS results show a clear evolution of the electronic structure upon annealing. The as-evaporated samples exhibit only a broad bump at approximately −2.5 eV binding energy showing no dispersion and increased spectral weight at E_F compared to the clean HOPG. Upon heating discrete bands appear which correspond well to an azimuthally integrated band structure calculation of bulk Pd with a (1 1 1) orientation.

Acknowledgements

We would like to thank P. Gröning, R. Fasel, and D. Naumović for fruitful discussions. Excellent technical assistance was provided by J. Frischknecht, C. Neururer, F. Bourqui, and the mechanical workshop under the leadership of E. Mooser and O. Raetzo. This work was supported by the Swiss National Science Foundation.

References

[1] Ch. Kuhrt, M. Harsdorff, Surf. Sci. 245 (1991) 173.
[2] I. Kojima, A.K. Srivastava, M. Kurahashi, Jpn. J. Appl. Phys. 30 (1991) 1852.
[3] C.M. Whelan, C.J. Barnes, Appl. Surf. Sci. 119 (1997) 288.
[4] A. Piednoir, E. Perrot, S. Granjeaud, A. Humbert, C. Chapon, C.R. Henry, Surf. Sci. 391 (1997) 19.
[5] A. Humbert, M. Dayez, S. Granjeaud, P. Ricci, C. Chapon, C.R. Henry, J. Vac. Sci. Technol. B 9 (1991) 804.
[6] M. Zinke-Allmang, L.C. Feldman, M.H. Grabow, Surf. Sci. Rep. 16 (1992) 377.
[7] P. Blaha, K. Schwarz, J. Luitz, WIEN97, Vienna University of Technology, Improved and updated UNIX version of the original copyrighted WIEN-code; P. Blaha, K. Schwarz, P. Sorantin, S.B. Trickey, Comput. Phys. Commun. 59 (1990) 399.
[8] J. Osterwalder, T. Greber, A. Stuck, L. Schlapbach, Phys. Rev. B 47 (1991) 13764.
[9] D. Naumović, A. Stuck, T. Greber, J. Osterwalder, L. Schlapbach, Phys. Rev. B 47 (1993) 7462.
[10] R. Fasel, P. Aebi, J. Osterwalder, L. Schlapbach, R.G. Agostino, G. Chiarello, Phys. Rev. B 50 (1994) 14516.
[11] Th. Pillo, L. Patthey, E. Boschung, J. Hayoz, P. Aebi, L. Schlapbach, J. Electr. Spectrosc. Relat. Phenom. 97 (1998) 243.
[12] Rasterscope™ 3000 UHV STM, Danish Micro Engineering (DME), DK-2730 Herlev, Denmark.
[13] H. Zabel, S.A. Solin (Eds.), Graphite Intercalation Compounds I, Springer Series in Materials Science 14, Springer, Berlin, 1990.
[14] C.S. Fadley, in: R.T. Bachrach (Ed.), Synchrotron Radiation Research: Advances in Surface Science, vol. 1, Plenum, New York, 1990.
[15] D. Naumović, Ph.D. Thesis, Physics Institute, University of Fribourg 1993.
[16] R.G. Agostino, O.M. Küttel, R. Fasel, J. Osterwalder, L. Schlapbach, Phys. Rev. B 49 (1994) 13820.
[17] M. Seelmann-Eggebert, H.J. Richter, Phys. Rev. B 43 (1991) 9578.
[18] M. Seelmann-Eggebert, R. Fasel, E.C. Larkins, J. Osterwalder, Phys. Rev. B 48 (1993) 11838.
[19] J.P. Perdew, S. Burke, M. Ernzerhof, Phys. Rev. Lett. 77 (1996) 3865.
[20] D.R. Lloyd, C.M. Quinn, N.V. Richardson, Surf. Sci. 63 (1977) 174.
[21] R. Nishitani, A. Kasuya, S. Kubota, Y. Nishina, J. Vac. Sci. Technol. B 9 (2) (1991) 806.
[22] T. Michely, M. Hohage, M. Bott, G. Comsa, Phys. Rev. Lett. 70 (1993) 3943.